De-embedding of Port Discontinuities in Full-Wave CAD Models of Multi-Port Circuits

V.I. Okhmatovski, J. Morsey, and A.C. Cangellaris

University of Illinois at Urbana-Champaign, Dept. of ECE, 1406 W. Green Str., Urbana, IL 61801, U.S.A, e-mail: okhmatov@uiuc.edu

Abstract — **Systematic numerical methodology is proposed for accurate de-embedding of the port discontinuities in full-wave models of the unbounded multi-port circuits. The approach is based on the idea of short-open calibration (SOC). The latter being a numerical analog of the experimental TRL-technique provides a consistent removal of the feed networks in a wide range of frequencies. The treatment of multi-port topologies is achieved through the continuation of the original scalar SOC into the vector space. The new vector short-open calibration (VSOC) method provides a seamless interface with the integral equation based method of moments (MoM) solvers. Owing to the distributed nature of the microwave circuits the method allows for a substantial flexibility in the choice of the excitation mechanisms. Such commonly used MoM driving schemes as the ports locally backed up by the vertical wall, ungrounded-internal differential ports or via-mounted ports can be accurately de-embedded within the framework of the VSOC.**

I. Introduction

The integral equation based method of moments has established itself as an accurate and efficient tool for simulation of the electromagnetic phenomena in complex microwave circuits merged into multi-layered environment. Independent of the implementation, the MoM requires de-embedding of the discontinuities introduced into the analysis by the ports and the transmission lines delivering the signal to the system. While the ports excite higher order fields, the transmission lines introduce an additional phase shift, impedance mismatch and loss. Aforementioned parasitics are to be de-embedded and the S-, Y- or Z-parameters for the principle TEM-mode are to be extracted. Among various techniques used for de-embedding, the extended bibliography for which can be found in [1], the methodology based on short-open calibration [1] has been demonstrated to provide higher accuracy and consistency of results in a wide range of frequencies [3]. Being a numerical analog of the TRL calibration technique widely used in the experimental microwave community, SOC methodology has a potential for very accurate wide-band removal of the error and parasistic terms brought into the analysis by the feed networks. The SOC method was originally proposed and developed for the two-ports devices [1]. In this paper we extend its capabilities to treat multi-port circuits by continuing the scalar currents and voltages into the vector space. Cascaded S-matrix formulation is adopted instead of using the transmission ABCD-matrices, which allows us to handle multi-port systems with different number of ports at the input and the output.

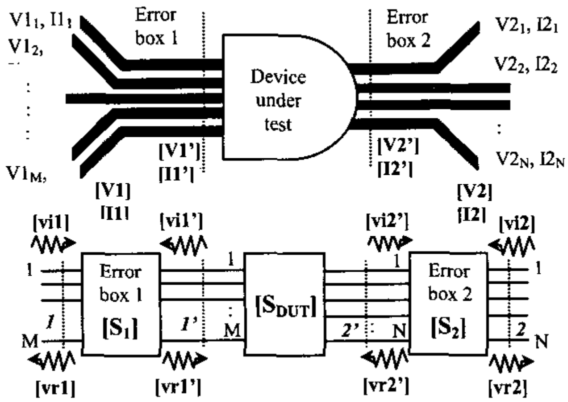

Fig. 1. Geometry of a multi-port device and its representation in terms of cascaded S-matrices

The original SOC technique [1] utilizes the impressed-field excitation model [2], where each port is excited by a δ-gap generator backed up by a locally attached PEC wall intended to provide the common ground reference for each port in the circuit. In this paper we demonstrate that that due to the distributed nature of the microwave devices, the concept of local grounds can be utilized at each port, allowing for elimination of the PEC walls from the analysis. This observation results in a significant simplification of the MoM implementation and removal of parasitic effects brought into analysis by the presence of the PEC walls.

II. Problem Statement

The geometry of a generalized arbitrary shaped microwave $(N+M)$- port device and its equivalent representation are sketched in Fig.1. The equivalent characterization of the device is presented as a cascade of

$\mathbf{S}$-matrices of the two error boxes and the device under test (DUT). The 'error boxes' represent the feeding networks, which are to be numerically de-embedded. From the theory of cascaded $\mathbf{S}$-matrices it is know that if the $\mathbf{S}_\Sigma$ of the entire cascade is available as well as the scattering parameters $\mathbf{S}_1$ and $\mathbf{S}_2$ of the error boxes, the desired $\mathbf{S}_{DUT}$-matrix of the device can be readily found through the algebraic manipulations with the submatrices of $\mathbf{S}_\Sigma$, $\mathbf{S}_1$ and $\mathbf{S}_2$ as discussed at the end of this Section.

Hence, the first step of the de-embedding procedure is to compute $\mathbf{Y}_\Sigma$- matrix using MoM as described in [2] and consequently the $\mathbf{S}_\Sigma$-matrix of the entire device including the feed circuits as

$$\mathbf{S}_\Sigma = (\mathbf{I} - \mathbf{Y}_\Sigma Z_0)\cdot(\mathbf{I} - \mathbf{Y}_\Sigma Z_0), \tag{1}$$

where Z_0 is some arbitrary reference impedance. Even though in [2] it is prescribed that the impressed-field excitation model including δ-gap generator backed up by a PEC wall is to be employed (Fig. 2a), one can also excite the system through the ungrounded-internal ports (Fig. 2b), through ports mounted on vias (Fig. 2c) or the combination of the latter two. We refer to the ungrounded-internal ports (Fig. 2b) as the locally-grounded ports where the local ground is represented by the open end of the transmission line stub hanging in the air. It is emphasized that the excitation mechanisms avoiding the usage of the PEC walls are preferable because the unwanted influence of the walls on the DUT is then eliminated.

The SOC technique is used next in order to obtain first the $\mathbf{ABCD}$-matrices of the feed lines and consequently their desired scattering parameters $\mathbf{S}_1$ and $\mathbf{S}_2$. The layout of the feeding network is mirrored with respect to the reference planes of the DUT as shown in Fig.3. The plane of symmetry allows simulation of the perfectly shorted termination (PEC wall) and perfectly open termination (PMC wall) for the error box at the reference plane. In order to achieve the perfect shorted or open termination, symmetric and anti-symmetric excitation must be applied respectively at the ports as shown in Fig. 3b and Fig. 3c. The same MoM code, which was used to compute $\mathbf{Y}_\Sigma$- matrix of the entire device, can be utilized now to evaluate the currents in the error box under the conditions of shorted and open terminations yielding the desired $[\mathbf{a}]$, $[\mathbf{b}]$, $[\mathbf{c}]$ and $[\mathbf{d}]$ blocks of a feed network transmission matrix. To elaborate let us write down the $\mathbf{ABCD}_1$ matrix of the first error box

$$\begin{bmatrix}[\mathbf{a1}] & [\mathbf{b1}]\\ [\mathbf{c1}] & [\mathbf{d1}]\end{bmatrix}\cdot\begin{bmatrix}[\mathbf{V1'}]\\ -[\mathbf{I1'}]\end{bmatrix} = \begin{bmatrix}[\mathbf{V1}]\\ -[\mathbf{I1}]\end{bmatrix} \tag{2}$$

where $[\mathbf{a1}]$, $[\mathbf{b1}]$, $[\mathbf{c1}]$ and $[\mathbf{d1}]$ are $(M\times M)$ matrices. In order to define blocks $[\mathbf{b1}]$ and $[\mathbf{d1}]$, M linearly independent symmetric excitations are applied at the input ports and their mirror counterparts, each of which ensures perfectly shorted termination at the plane of symmetry (Fig. 3). Consequently, from (2) $[\mathbf{V1S'}] = [\mathbf{0}]$ and $-[\mathbf{b1}]\cdot[\mathbf{I1S'}] = [\mathbf{V1S}]$ hold true and can be rewritten in the explicit form as

$$-\begin{bmatrix} b1_{11} & b1_{12} & \cdots & b1_{1M}\\ b1_{21} & b1_{22} & \cdots & b1_{2M}\\ \vdots & \vdots & \ddots & \vdots\\ b1_{M1} & b1_{M2} & \cdots & b1_{MM}\end{bmatrix}\cdot\begin{bmatrix} I1S'_{11} & I1S'_{12} & \cdots & I1S'_{1M}\\ I1S'_{21} & I1S'_{22} & \cdots & I1S'_{2M}\\ \vdots & \vdots & \ddots & \vdots\\ I1S'_{M1} & I1S'_{M2} & \cdots & I1S'_{MM}\end{bmatrix}$$

$$= \begin{bmatrix} V1S_1 & 0 & \cdots & 0\\ 0 & V1S_2 & \cdots & 0\\ \vdots & \vdots & \ddots & \vdots\\ 0 & 0 & \cdots & V1S_M\end{bmatrix} \tag{3}$$

where the letters "S" and "O" are added to the notations in order to distinguish the shorted and the open termination modes respectively. $I1S'_{ij}$ is the current at the i-th reference plane port of the error box under symmetric j-th excitation, that is $[\mathbf{V1S}]^T = \begin{bmatrix}0 & \cdots & V1S_j & \cdots & 0\end{bmatrix}$. Inverting matrix $[\mathbf{I1S'}]$ and assuming $V1S_j = 1Volt$ for any j, we compute submatrix $[\mathbf{b1}]$ as

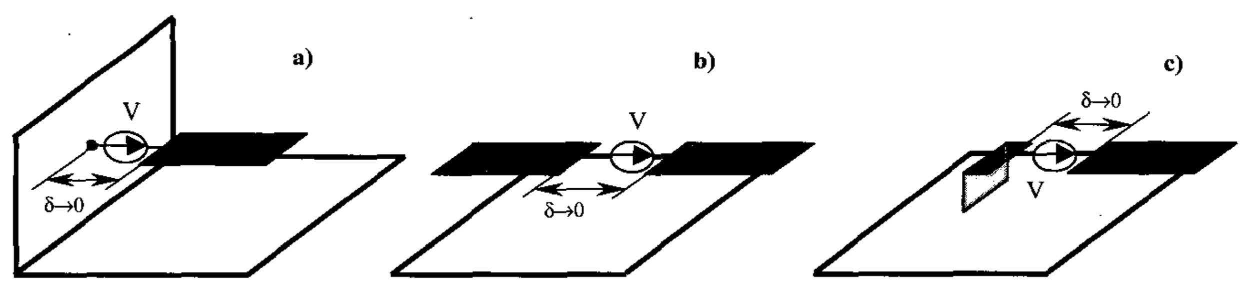

Fig. 2. Excitation models: a) Wall-backed port, b) Ungrounded-internal port, c) Via port

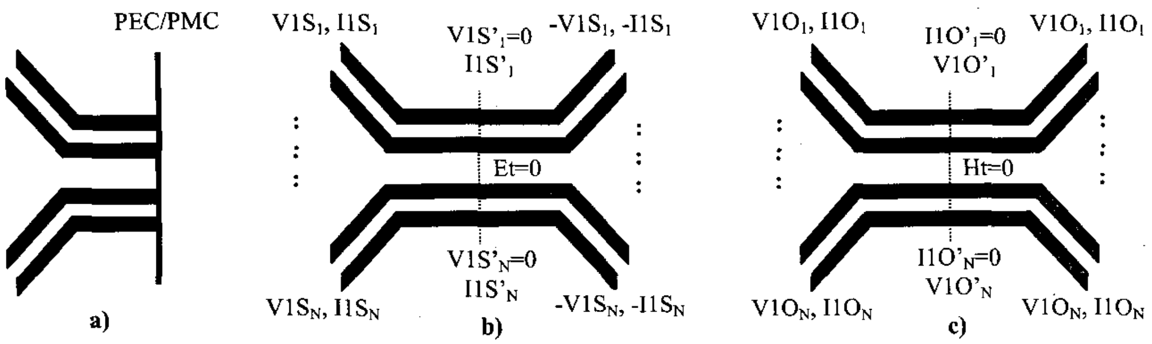

Fig. 3. Physical model and a pair of symmetrically and anti-symmetrically excited structures for the 3D MoM algotithm. (a) Physical model. (b) Ideal short termination. (c) Ideal open termination.

$$[\mathbf{b1}] = -[\mathbf{I1S'}]^{-1}. \tag{4}$$

From the same MoM solution for the shorted termination and the same M linearly independent excitations $[\mathbf{V1S}]$, we obtain the matrix of currents $[\mathbf{I1S}]$ at the input ports of the error box. Then the matrix block $[\mathbf{d1}]$ can be readily obtained as follows

$$[\mathbf{d1}] = -[\mathbf{I1S}]\cdot[\mathbf{I1S'}]^{-1}. \tag{5}$$

Similarly, employing M linearly independent anti-symmetric excitations at the port of the error box (Fig. 3c), which simulate perfectly open termination $[\mathbf{I1O'}] = [\mathbf{0}]$, from (2) we get $[\mathbf{a1}] = [\mathbf{V1O'}]^{-1}\cdot[\mathbf{V1O}]$, $[\mathbf{c1}] = [\mathbf{I1O}]\cdot[\mathbf{V1O'}]^{-1}$. The excitation voltages $[\mathbf{V1O}]$ can be assumed to be the identity matrix having dimension $[Volt]$. Since from the MoM solution we do not know how to measure voltages $[\mathbf{V1O'}]$ at the open termination but can easily measure currents $[\mathbf{I1O}]$ at the input ports, we would like to exclude voltages $[\mathbf{V1O'}]$ from the analysis and rewrite expressions for submatrices $[\mathbf{a1}]$ and $[\mathbf{c1}]$ only in terms of the currents $[\mathbf{I1S}]$, $[\mathbf{I1S'}]$ and $[\mathbf{I1O}]$. For this purpose the relation $[\mathbf{a1}][\mathbf{d1}]-[\mathbf{c1}][\mathbf{b1}] = [\mathbf{I}]$ is utilized providing, after some algebra manipulations, the desired formulae for the submatrices $[\mathbf{a1}]$ and $[\mathbf{c1}]$

$$\begin{aligned}[\mathbf{a1}] &= [\mathbf{I1S'}]\cdot([\mathbf{I1O}]-[\mathbf{I1S}])^{-1}, \\ [\mathbf{c1}] &= [\mathbf{I1O}]\cdot[\mathbf{I1S'}]\cdot([\mathbf{I1O}]-[\mathbf{I1S}])^{-1}.\end{aligned} \tag{6}$$

In order to obtain the scattering matrix $\mathbf{S}_1$ of the first error box its transmission matrix is converted first to the admittance matrix $\mathbf{Y}_1$

$$\begin{bmatrix}\mathbf{Y}_{11} & \mathbf{Y}_{11'} \\ \mathbf{Y}_{1'1} & \mathbf{Y}_{1'1'}\end{bmatrix} = \begin{bmatrix}[\mathbf{d1}]\cdot[\mathbf{b1}]^{-1} & [\mathbf{c1}]-[\mathbf{d1}]\cdot[\mathbf{b1}]^{-1}\cdot[\mathbf{a1}] \\ -[\mathbf{b1}]^{-1} & [\mathbf{b1}]^{-1}\cdot[\mathbf{a1}]\end{bmatrix}. \tag{7}$$

Then, using the same reference impedance Z_0 introduced in (1) the scattering matrix of the first error box can be evaluated as $\mathbf{S}_1 = (\mathbf{I}-\mathbf{Y}_1 Z_0)\cdot(\mathbf{I}-\mathbf{Y}_1 Z_0)$. In a similar fashion the scattering parameters $\mathbf{S}_2$ of the second error box can be computed using the MoM and vector SOC.

Once the scattering matrices $\mathbf{S}_1$ and $\mathbf{S}_2$ of the feed networks are obtained as well at the $\mathbf{S}_\Sigma$-matrix of the entire device the de-embedding of the error boxes can be done in a successive manner as explained below. Let us denote the scattering matrix of the DUT cascaded with the second error box as $\mathbf{S}_{DUT2}$ Then, the following relations between the incident and reflected normalized voltage wave amplitudes hold true

$$\begin{aligned}[\mathbf{vr1}] &= [\mathbf{S}_\Sigma^{11}]\cdot[\mathbf{vi1}]+[\mathbf{S}_\Sigma^{12}]\cdot[\mathbf{vi2}], \\ [\mathbf{vr2}] &= [\mathbf{S}_\Sigma^{21}]\cdot[\mathbf{vi1}]+[\mathbf{S}_\Sigma^{22}]\cdot[\mathbf{vi2}], \\ [\mathbf{vr1}] &= [\mathbf{S}_1^{11}]\cdot[\mathbf{vi1}]+[\mathbf{S}_1^{11'}]\cdot[\mathbf{vi1'}], \\ [\mathbf{vr1'}] &= [\mathbf{S}_1^{1'1}]\cdot[\mathbf{vi1}]+[\mathbf{S}_1^{1'1'}]\cdot[\mathbf{vi1'}].\end{aligned} \tag{8}$$

where $[\mathbf{vi}]+[\mathbf{vr}] = [\mathbf{V}]/\sqrt{Z_0}$, $[\mathbf{vi}]-[\mathbf{vr}] = [\mathbf{I}]\sqrt{Z_0}$.

Eliminating vectors $[\mathbf{vi1}]$ and $[\mathbf{vr1}]$ from (8) we get two matrix equation for the submatrices of $\mathbf{S}_{DUT2}$

$$\begin{aligned}[\mathbf{vi1'}] &= [\mathbf{S}_{DUT2}^{1'1'}]\cdot[\mathbf{vr1'}]+[\mathbf{S}_{DUT2}^{1'2}]\cdot[\mathbf{vi2}], \\ [\mathbf{vr2}] &= [\mathbf{S}_{DUT2}^{21'}]\cdot[\mathbf{vr1'}]+[\mathbf{S}_{DUT2}^{22}]\cdot[\mathbf{vi2}],\end{aligned} \tag{9}$$

matrix blocks of $\mathbf{S}_{DUT2}$ being

$$\begin{aligned}[\mathbf{S}_{DUT2}^{1'1'}] &= ([\mathbf{S}_1^{1'1'}]+[\mathbf{S}_1^{1'1}]\cdot([\mathbf{S}_\Sigma^{11}]-[\mathbf{S}_1^{11}])^{-1}\cdot[\mathbf{S}_1^{11'}])^{-1}, \\ [\mathbf{S}_{DUT2}^{1'2}] &= ([\mathbf{S}_1^{11'}]\cdot([\mathbf{I}]-[\mathbf{S}_{DUT2}^{1'1'}]\cdot[\mathbf{S}_1^{1'1'}])^{-1})^{-1}\cdot[\mathbf{S}_\Sigma^{12}], \\ [\mathbf{S}_{DUT2}^{21'}] &= [\mathbf{S}_\Sigma^{21}]\cdot(([\mathbf{I}]-[\mathbf{S}_1^{1'1'}]\cdot[\mathbf{S}_{DUT2}^{1'1'}])^{-1}\cdot[\mathbf{S}_1^{1'1}])^{-1}, \\ [\mathbf{S}_{DUT2}^{22}] &= [\mathbf{S}_\Sigma^{22}]-[\mathbf{S}_{DUT2}^{21'}]\cdot([\mathbf{I}]-[\mathbf{S}_1^{1'1'}]\cdot[\mathbf{S}_{DUT2}^{1'1'}])^{-1}\cdot[\mathbf{S}_1^{1'1'}]\cdot[\mathbf{S}_{DUT2}^{1'2}].\end{aligned} \tag{10}$$

Evaluation of $\mathbf{S}_{DUT2}$ is equivalent to the de-embedding of the first error box. Similarly, considering the matrix $\mathbf{S}_{DUT2}$ as a cascade of the DUT scattering matrix $\mathbf{S}_{DUT}$ and $\mathbf{S}_2$ the de-embedding of the second error box is performed yielding the desired $\mathbf{S}_{DUT}$.

II. NUMERICAL RESULTS

In order to validate the proposed methodology various multi-port circuits were considered. The method demonstrated robustness and the ability to provide high-accuracy de-embedding for different multiport topologies. The example we consider in this paper is the transition from three to two transmission lines which geometry and MoM discretization are shown in Fig. 4 for the case of 2.5mm long feed lines. The internal ungrounded ports (Fig. 2b) with the local ground references were used to drive the circuits (shown with thick vertical lines at the ends of the conductors). The circuit is printed on top of the grounded dielectric layer of thickness 0.7mm and relative permittivity $\varepsilon_r = 3$. The thickness of conductors was assumed to be infinitely small. De-embedding of the error boxes was performed for three different lengths of the feed networks L=2.5mm, 3.5mm and 5mm. The de-embedded scattering parameters of the device for the case when the circuit is driven through the first port are presented in Fig. 5. The S - parameters obtained as a result of de-embedding of the different feed networks agree very well in a wide range of frequencies testing the method to be effective and accurate. To provide an independent reference the same circuit was simulated with the Sonnet EM software. The corresponding S - parameters are ploted on the same figure. Our simulation results compare very well with the ones generated by Sonnet and through several numerical examples we observed a better accuracy of de-embedding provided through the vector short-open calibration especially for the weakly coupled ports of the device. This behavior is consistent with the comparative study done in [3].

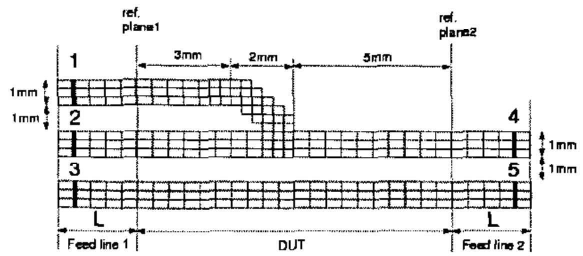

Fig. 4. Geometry and MoM discretization of the transition from three to two transmission lines

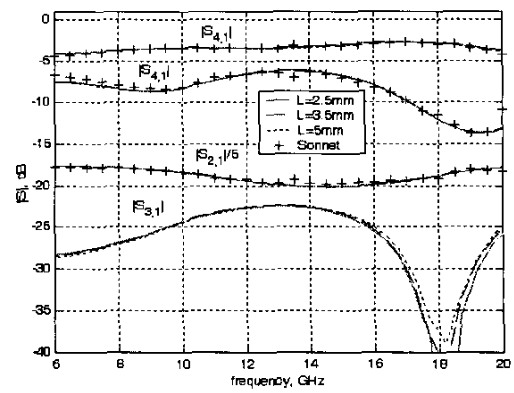

Fig. 5. Scattering parameters of the 3-to-2 transition.

III. CONCLUSION

In this paper an accurate and systematic methodology has been presented and validated for the wide-band numerical de-embedding of the network parameters in full-wave CAD models of multi-port microwave devices. The method is based on the idea of short-open calibration extended into the vector space to accommodate for the multi-port circuit topologies. This technique provides a seamless interface with the integral equation based MoM numerical schemes and is free of inconsistencies between 2D transmission feed line models and 3D full-wave circuit model typically attributed to the conventional de-embedding methods. It is demonstrated that due to the distributed nature of the microwave circuits a substantial flexibility in the choice of the numerical excitation mechanisms can be exercised making PEC walls backing up the δ-gap generators redundant and avoidable.

ACKNOWLEDGEMENT

This work was supported by the DARPA NeoCAD program and the Semiconductor Research Corporation.

REFERENCES

[1] Lei Zhu and Ke Wu, "Unified Equivalent-Circuit Model of Planar Discontinuities Suitable for Field Theory-Based CAD and Optimization of M(H)MIC", *IEEE Trans. Microwave Theory and Tech.*, Vol. MTT-47, pp. 1589-1602, Sept. 1999.

[2] G.V. Eleftheriades and J.R. Mosig, "On the Network Characterization of Planar Passive Circuits Using the Method of Moments", *IEEE Trans. Microwave Theory and Tech.*, Vol. MTT-44, pp. 438-445, Mar. 1996.

[3] Lei Zhu and Ke Wu, "Comparative investigation on numerical de-embedding techniques for equivalent circuit modeling of lumped and distributed microstrip circuits", *IEEE Microwave and Wireless Components Lett.*, Vol. 12, pp. 51-53, Feb. 2002.